Journal of proteome research

Article

pubs.acs.org/jpr

Resveratrol-Induced Changes of the Human Adipocyte Secretion Profile

Anja Rosenow,*[,†] Jean-Paul Noben,[‡] Johan Jocken,[†] Sonja Kallendrusch,[†] Pamela Fischer-Posovszky,[§] Edwin C.M. Mariman,[†] and Johan Renes[†]

[†]Department of Human Biology, NUTRIM School for Nutrition, Toxicology and Metabolism, Maastricht University, Maastricht, The Netherlands

[‡]Biomedical Research Institute, Hasselt University, and School of Life Sciences, transnationale Universiteit Limburg, Diepenbeek, Belgium

[§]Endocrine Research Laboratory, Division of Pediatric Endocrinology and Diabetes, Ulm University Medical Center, Germany

Supporting Information

ABSTRACT: Enlarged white adipose tissue (WAT) is a feature of obesity and leads to changes in its paracrine and endocrine function. Dysfunction of WAT cells is associated with obesity-associated disorders like type 2 diabetes and cardiovascular diseases. Resveratrol (RSV), a natural polyphenolic compound, mimics beneficial effects of calorie restriction. As such, RSV seems a promising therapeutic target for obesity-associated disorders. The effect of RSV on the human adipokine profile is still elusive. Therefore, a proteomic study together with bioinformatical analysis was performed to investigate the effect of RSV on the secretion profile of mature human SGBS adipocytes. RSV incubation resulted in elevated basal glycerol release and reduced intracellular TG content. This increased intracellular lipolysis was accompanied by profound changes in the adipocyte secretion profile. Extracellular matrix proteins were down-regulated while processing proteins were mostly up-regulated after RSV treatment. Interestingly, RSV induced secretion of proteins protective against cellular stress and proteins involved in the regulation of apoptosis. Furthermore, we found a RSV-induced up-regulation of adiponectin and ApoE accompanied by a down-regulation of PAI-1 and PEDF secretion which may improve anti-inflammatory processes and increased insulin sensitivity. These effects may contribute to alleviate obesity-induced metabolic complications. In addition, two novel RSV-regulated adipocyte-secreted proteins were identified.

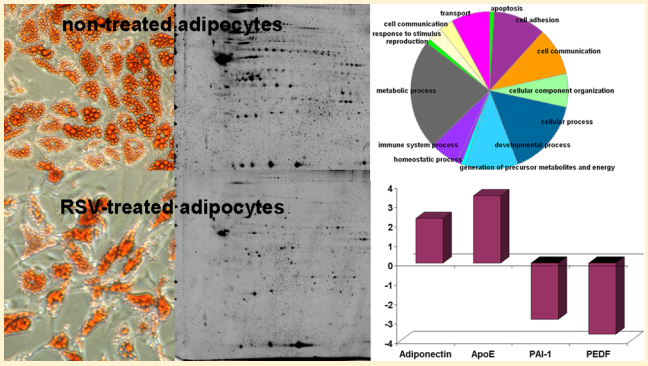

KEYWORDS: *human adipocytes, RSV, adipokines, lipolysis, 2-DE LC−MS/MS,*

INTRODUCTION

The polyphenol resveratrol (RSV) (3,4′,5-trihydroxystilbene) is synthesized in more than 70 plant species and is present in many dietary substances.[1,2] Animal studies have shown that RSV mimics several beneficial effects of calorie restriction including prevention of insulin resistance, increased mitochondrial contents of several tissues like liver and skeletal muscles as well as the restoration of normal longevity in obese mice.[1,3,4] However, despite other benefits from calorie restriction, such as slowing heart rate, prevention of spontaneous lymphomas, and decreased core body temperature, RSV-treatment did not extend the lifespan in nonobese animals.[1,3,4] Recently, Timmers et al.[5] and Olholm et al.[6] have demonstrated that RSV can mimic positive effects of calorie restriction in obese humans. These included improvement of insulin resistance, decreased levels of blood glucose, triglycerides and cytokines as well as decreased intramyocellular lipid levels, decreased intrahepatic lipid content, and decreased systolic blood pressure.[5,6] However, the molecular pathways by which RSV executes its beneficial effect are still poorly known.

In mammals, most of the beneficial effects of RSV treatment are mediated by the activation of sirtuin (SIRT) 1.[7] SIRT1 is the mammalian homologue of the yeast Sir2 protein, which is involved in the longer lifespan of yeast upon calorie restriction.[8] However, it is still under discussion if RSV activates SIRT1 in a direct or indirect manner. Recently published data demonstrate a SIRT1 activation as a downstream signaling effect of a RSV-stimulated AMP-activated protein kinase (AMPK) activation[1,9] In addition, Park et al.[10] showed cAMP effector protein Epac1 as a key regulator of the RSV-induced effects which in turn activates AMPK and SIRT1.

Obesity and its associated diseases like type 2 diabetes, cardiovascular complications and certain cancers are currently

Received: June 16, 2012
Published: August 20, 2012

major health burdens. Obesity is characterized by morphological, histological and functional changes of accumulated white adipose tissue (WAT). The accumulation of WAT is associated with an increase of adipocyte number (hyperplasia) and/or with an enlargement of existing adipocytes (hypertrophy).[11] Simultaneously, changes of the paracrine and endocrine functions of WAT are related to changes in the protein expression and secretion profiles of (pre)adipocytes. Hormones, cytokines, neurotrophins, extracellular matrix proteins as well as proteins involved in angiogenesis, inflammation, lipid and glucose metabolism are known secreted factors of WAT and a dysregulation of their secretion pattern may lead to obesity-associated disorders.[12,13]

Previously, we investigated changes in the secretion profiles during fat cell differentiation by using human Simpson Golabi Behmel Syndrome (SGBS) adipocytes.[14] Here we hypothesized that RSV may have a beneficial effect on the secretion profile of mature human SGBS adipocytes. Therefore, the differences of the secretome of fully differentiated RSV-treated or nontreated SGBS adipocytes were analyzed by two-dimensional gel electrophoresis (2-DE). The identification of the secreted proteins was performed by liquid chromatography−electrospray ionization tandem mass spectrometry (LC−ESI−MS/MS).

EXPERIMENTAL SECTION

Materials

Culture media, 0.5% trypsin-EDTA and 10 000 u/mL Penicillin/Streptomycin were obtained from Life Technologies (Bleiswijk, The Netherlands). Fetal bovine serum (FBS) was purchased from Bodinco (Alkmaar, The Netherlands). Additional cell culture supplements, RSV, protease inhibitor cocktail, phenylmethylsulfonylfluoride (PMSF), DL-dithiothreitol (DTT), 3-[(3-cholamidopropyl) dimethyl-amonio]-1-propanesulfonate (CHAPS), α-cyano-4-hydroxyl-cinnamic acid (CHCA), trifluoroacetic acid (TFA) and acetonitrile (ACN) were obtained from Sigma-Aldrich (Zwijndrecht, The Netherlands). Immobilized pH gradient (IPG) buffer (pH 3−11, nonlinear), Dry-Strip cover fluid and immobiline Dry-Strips (pH 3−11 nonlinear, 24 cm) were purchased from GE Healthcare (Diegem, Belgium).

Cell Culture

Human Simpson-Golabi-Behmel syndrome (SGBS) cells were obtained from Prof. Dr. M. Wabitsch (University of Ulm, Germany)[15] and cultured as described.[14] Ninety percentconfluent preadipocytes [$(2.2 \pm 0.36) \times 10,^6$ mean ± SEM, $n = 3$] were differentiated into mature adipocytes during 13 days as described.[14] On average, 83% of the preadipocytes differentiated into mature adipocytes. To determine cell numbers, adipocytes were counted with a raster ocular. Preadipocytes were trypsinized and counted with a hemocytometer. The number of adipocytes per 150 mm Petri dish was $(1.8 \pm 0.95) \times 10^6$ (mean ± SEM, $n = 7$).

RSV Experiments

Dose−response experiment was performed to define the optimal RSV concentration to study its effect on the human adipocyte secretome. Briefly, 13 days differentiated adipocytes were treated with 66 nM insulin and with different RSV concentrations (0, 5, 50, 75, 100, and 200 μM) in phenol red free DMEM/F12 medium for a period of 48 h. To study RSV-induced changes in the adipocyte secretome, fully differentiated adipocytes were washed twice with PBS and incubated for 48 h in phenol red free DMEM/F12 medium with 66 nM insulin and 75 μM RSV. Control adipocytes were cultured in a similar manner with 66 nM insulin and an equal volume of dimethylsulfoxide (DMSO) instead of RSV.

Effect of RSV on Lipolysis

To determine the effect of 48 h RSV treatment (75 μM) on intracellular lipolysis in human SGBS adipocytes, intracellular triglyceride (TG) content and glycerol release (marker of complete TG hydrolysis) were determined. Adipocytes were fixed with 3.7% formaldehyde for 10 min at room temperature. Fixed cells were incubated with a filtered Oil Red O (ORO) solution (1% ORO in 60% isopropyl alcohol) for 30 min. Finally, cells were washed 6 times with 70% ethanol. Images were taken with a Nikon TE 200 eclipse phase contrast microscope equipped with digital image acquisition. To determine intracellular TG accumulation, the ORO stain was extracted with DMSO and measured by spectrophotometry at 540 nm. The amount of intracellular ORO content was expressed per number of cells.

Glycerol in the culture medium was measured by a fluorimetric assay using a Cobas-Fara Instrument (Roche Diagnostics, Almere, The Netherlands). The amount of glycerol release was expressed per number of cells.

Sample Preparation of 2-DE Experiments

Culture media were collected, supplemented with protease inhibitor cocktail, transferred to dialysis tubes (2-kDa molecular-weight cutoff, Carl Roth GmbH, Karlsruhe, Germany) and dialyzed against 20 mM ammonium bicarbonate at 4 °C for 48 h with 10−12× buffer changes. The dialyzed medium samples were freeze-dried, dissolved in fresh rehydration buffer (8 M urea, 2% w/v CHAPS and 65 mM DTT) and centrifuged at 20 000*g* at 10 °C for 30 min. The protein concentrations were determined with a Bradford-based protein assay kit (Bio-Rad Laboratories). All samples were stored at −80 °C.

2-DE

Protein samples derived from 1.8×10^6 cells were used for 2-DE gel analysis according to Bouwman et al.[16] but with different IPG strips (pH 3−11 nonlinear, 24 cm). Total protein (100 μg) in a volume of 450 μL containing 0.5% (v/v) IPG buffer was loaded onto the IPG strips. For protein profiling, 5 independent replicates were made for RSV-treated and nontreated adipocytes. The gels were stained with Flamingo fluorescent gel stain according to the manufacturer's protocol (Bio-Rad Laboratories) and scanned by the Molecular Imager FX (Bio-Rad Laboratories) to visualize the proteins.

Image Analysis

Stained gels were processed by PDQuest 8.0 (Bio-Rad Laboratories). Data were normalized with respect to the total density of the gel image. The groups of RSV-treated and nontreated adipocytes were formed from samples of independent experiments with the same treatments. Protein spots were regarded as significantly differentially expressed if the average spot intensity between the groups differed more than 1.5-fold with $p < 0.05$ (Student's t test). The criteria for indicating a trend was a spot intensity difference of more than 1.5-fold and $0.05 < p < 0.1$. For subsequent protein identification, gels with differentially expressed spots were restained with SYPRO Ruby Protein Stain according to the manufacturer's protocol (Bio-Rad Laboratories).

dx.doi.org/10.1021/pr300539b | J. Proteome Res. 2012, 11, 4733−4743

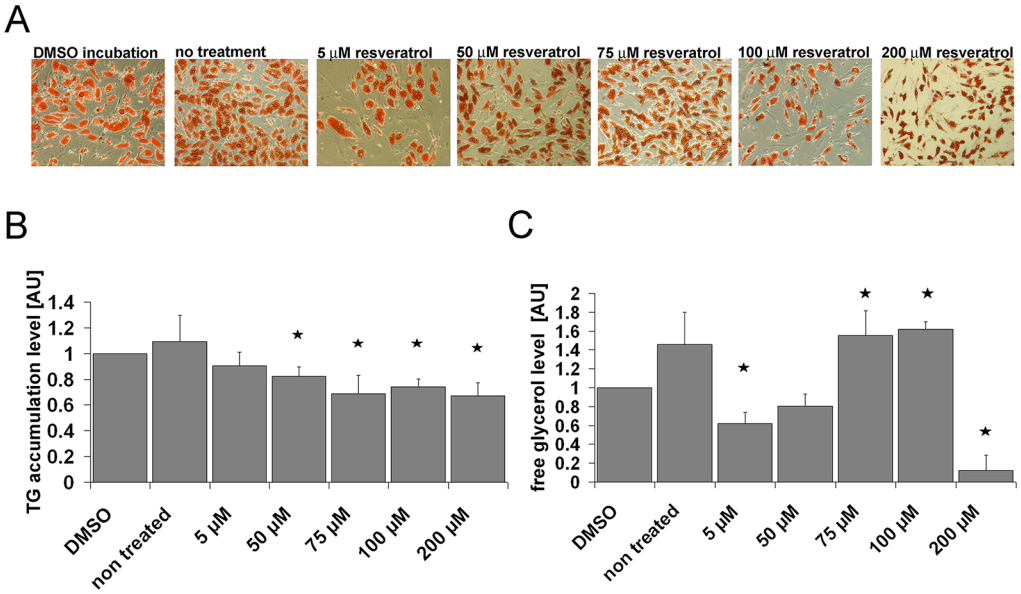

Figure 1. TG accumulation and glycerol release studies of RSV-treated SGBS adipocytes. (A) Images of 13 days differentiated adipocytes which were incubated for 48 h with different RSV concentrations. From left to right: incubation with DMSO (control), no treatment, incubation with 5, 50, 75, 100, and 200 μM RSV. Intracellular TG was stained by ORO and visualized by phase contrast microscopy. (B) Intracellular TG accumulation corrected for cell number determined by spectrophotometry after similar conditions as in panel A. (C) Glycerol release in the culture medium corrected for cell number determined after similar conditions as in panel A. Reported values are means ± SEM of 4 independent biological replications and * indicates differences with $p < 0.05$.

MS/MS and Protein Identification

Excised spots were in-gel digested as described by Bouwman et al.[16] Ten microliters of the digested spots was analyzed by LC−ESI−MS/MS on a LCQ Classic (ThermoFinnigan, San Jose, CA), as described by Dumont et al.[17] The trapped sample was separated on the analytical column (Biosphere C18, 5 μm particle diameter, 200 mm L × 0.05 mm i.d.; Nanoseparations, Nieuwkoop, The Netherlands) using a linear gradient from 5 to 60% (v/v) ACN in water containing 100 mM acetic acid in 55 min (100 nL/min). The eluate of the analytical column was nanosprayed from a Teflon-connected, gold-coated fused silica emitter (5 μm i.d.; NanoSeparations).

Database Search

With respect to LC−ESI−MS/MS, LCQ Xcalibur v2.0 SR2 raw files and spectra were selected from Proteome Discover1.2 software (Thermo Scientific) with the following settings: minimal peak count 50; total intensity threshold 4000; and S/N ≥ 6. Peak lists were searched with Sequest v1.2.0.208 and Mascot v2.3.0.1 against EMBL-EBI International Protein Index database for human proteins (version 3.78, 86 702 entries) and using following settings: fragment tolerance, 1.00 Da (monoisotopic); parent tolerance, 3.0 Da (monoisotopic); fixed modifications, carbamidomethylation of cystein; variable modifications, oxidation of methionin; max missed cleavages, 2. Search engine results were combined and validated by Scaffold v3.00.07 (Proteome Software, Portland, OR) with minimum peptide and protein probability set to ≥80%, followed by visual inspection of spectral (annotation) quality and manual curation, eliminating high-background spectra and single-engine identifications, evaluating one-hit wonders and filtering out keratins. Finally, the Mascot DAT files were processed by PRIDE Converter software[18] and were submitted together with relevant files (.raw, .mgf, .dat and Scaffold .sf3 files) via ProteomeXchange (http://www.proteomexchange.org) to the PRIDE database,[19] project accession number is 27081. Mass spectrometry data can be visualized using PRIDE Inspector[20] (http://tinyurl.com/csffalc) and Scaffold .sf3 free viewer (https://proteomecommons.org/tool.jsp?i=1009).

Analysis of Secreted Protein Candidates

For verification of secreted protein candidates, an amino acid sequence analysis was performed with SignalP 3.0 and SecretomeP 2.0 (CBS, Technical University Copenhagen, Denmark, www.cbs.tdu.dk). SignalP 3.0 was used to verify the presence and location of signal peptide cleavage sites in amino acid sequences. SecretomeP 2.0 was applied to categorize proteins as nonclassical secreted in case they are devoid of a signal peptide but obtain an NN-score above the threshold of 0.5.

Statistical Validation

All statistical analyses were performed with the Student's test. Significant differences between groups are indicated when $p < 0.05$.

RESULTS

RSV-Induced Lipolysis in Human SGBS Adipocytes

To investigate the RSV-induced secretome changes of mature SGBS adipocytes, the optimal RSV concentration was determined by which the highest TG hydrolysis and the lowest apoptotic stress response were observed. This was measured by intracellular TG content and glycerol release. A significant reduction of TG was observed with RSV treatment of 50 μM and higher (Figure 1A,B). A significant increase of glycerol release was observed with 75 μM and 100 μM RSV treatment (Figure 1C). Incubation with 200 μM RSV showed a strong reduction of intracellular TG but this was together with a significant decrease of glycerol release which may indicate cytotoxic effects (Figure 1A−C). According to these results, we choose a RSV concentration of 75 μM which was the lowest

dx.doi.org/10.1021/pr300539b | J. Proteome Res. 2012, 11, 4733−4743

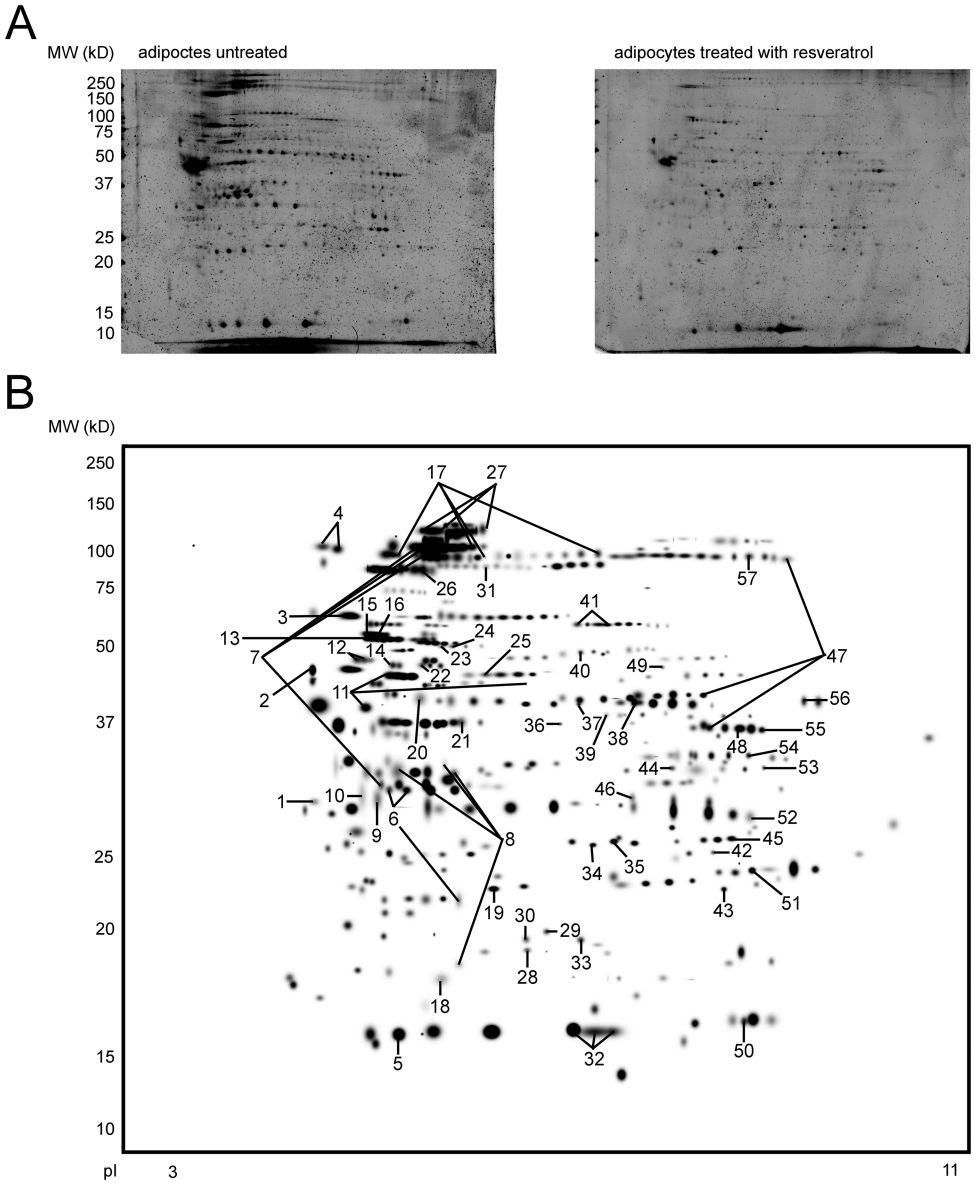

Figure 2. 2-DE gels of SGBS adipocyte secreted proteins. (A) Representative gels of medium-derived secreted proteins of 13 days differentiated SGBS adipocytes in the absence (left) or presence (right) of 75 μM RSV. (B) Master gel with identified spots. Spot numbers refer to ID numbers in Table 1.

concentration that produced a significant TG reduction and glycerol release (Figure 1).

Secretome Analysis of RSV-Treated Adipocytes

Changes in the secretome were determined by comparing 100 μg protein samples derived from 13-day differentiated adipocytes, treated for 48 h with 75 μM RSV or with DMSO (control). Proteins were separated by 2-DE and analyzed by PDQuest. Representative gels of the control and RSV condition, together with the master gel are shown in Figure 2.

From a total of 484 matched spots, 155 spots were significantly ($p > 0.05$) (112) or as trend ($p > 0.1$) (43) differentially expressed. These spots were excised from the gels and analyzed by LC–ESI–MS/MS. Eighty-one of the 155 spots were identified, which revealed 57 unique proteins. These 57 proteins were analyzed by SignalP 3.0 and Secretome 2.0 which revealed 26 proteins as classical secreted proteins, 14 proteins as nonclassical secreted and 17 proteins annotated as intracellular proteins. The category of classical secreted proteins is further subcategorized into extracellular matrix (ECM) proteins, processing proteins and regulation/signaling proteins (Figure 2, Table 1, Supporting Information File 1).

The 17 intracellular proteins are mostly associated with cell death or cell leakage. However, they were mainly identified within spots containing more than one protein, and as such, they are listed in the context of spot regulation. The ECM proteins including collagens, EGF-containing fibulin-like extracellular matrix protein 1, fibronectin, laminin and nidogen-2 were significantly or by trend down-regulated. In addition, nonclassical secreted proteins related to cellular structure components including serpin H1 and vimentin were significantly down-regulated. Most of the processing proteins including cathepsin L1, cystatin C, complement factor D (by trend) and procollagen C-endopeptidase enhancer 1 were significantly induced by RSV. Further analysis of the identified proteins revealed that RSV similarly regulated proteins associated with cell stress (putative heat shock 70 kDa protein

dx.doi.org/10.1021/pr300539b | J. Proteome Res. 2012, 11, 4733–4743

Table 1. Identification of Secreted Proteins from RSV-Treated or Nontreated SGBS Adipocytes by 2-DE Followed by LC−MS/MS[a]

accession number	protein name		ID	MW [kDa]	fold change	treatment *p*-value
		Classical Secreted				
		Extracellular Matrix				
P27797	Calreticulin		2	70.3	3.3×10^{0}	6.17×10^{-2}
P02452	**Collagen alpha-1(I) chain**	C-term	7	35.8	-1.9×10^{0}	7.35×10^{-2}
			7	**243.4**	$\mathbf{-2.1 \times 10^{5}}$	$\mathbf{2.64 \times 10^{-2}}$
			7	249.1	-3.8×10^{1}	5.49×10^{-2}
			7	**249.2**	$\mathbf{-4.3 \times 10^{0}}$	$\mathbf{4.75 \times 10^{-2}}$
			17	**246.2**	$\mathbf{-2.6 \times 10^{5}}$	$\mathbf{4.94 \times 10^{-6}}$
			17	**249.7**	$\mathbf{-5.6 \times 10^{0}}$	$\mathbf{3.29 \times 10^{-2}}$
			17	**241.0**	$\mathbf{5.8 \times 10^{0}}$	$\mathbf{7.54 \times 10^{-3}}$
			17	244.5	-2.8×10^{0}	6.33×10^{-2}
P02461	**Collagen alpha-1(III) chain**	C-term	**6**	**34.9**	$\mathbf{-9.4 \times 10^{4}}$	$\mathbf{2.28 \times 10^{-5}}$
		C-term	**6**	**34.9**	$\mathbf{-1.7 \times 10^{0}}$	$\mathbf{4.46 \times 10^{-2}}$
		C-term	**6**	**21.0**	$\mathbf{-3.8 \times 10^{4}}$	$\mathbf{9.40 \times 10^{-7}}$
		C-term	7	35.8	-1.9×10^{0}	7.35×10^{-2}
			7	**243.4**	$\mathbf{-2.1 \times 10^{5}}$	$\mathbf{2.64 \times 10^{-2}}$
			7	249.1	-3.8×10^{1}	5.49×10^{-2}
			7	**249.2**	$\mathbf{-4.3 \times 10^{0}}$	$\mathbf{4.75 \times 10^{-2}}$
P12109	Collagen alpha-1(VI) chain		26	209.6	6.4×10^{0}	6.29×10^{-2}
P08123	**Collagen alpha-2(I) chain**		**57**	**242.1**	$\mathbf{-4.7 \times 10^{0}}$	$\mathbf{1.24 \times 10^{-2}}$
P12110	Collagen alpha-2(VI) chain (isoform 2C2)		31	221.3	3.2×10^{0}	9.10×10^{-2}
Q12805	**EGF-containing fibulin-like extracellular matrix protein 1(isoform 1)**		**12**	**79.1**	$\mathbf{-2.2 \times 10^{5}}$	$\mathbf{7.29 \times 10^{-3}}$
			12	**79.0**	$\mathbf{-7.1 \times 10^{4}}$	$\mathbf{2.45 \times 10^{-4}}$
P02751	**Fibronectin**		**27**	**263.8**	$\mathbf{-2.8 \times 10^{4}}$	$\mathbf{1.10 \times 10^{-2}}$
			27	**263.2**	$\mathbf{-3.1 \times 10^{5}}$	$\mathbf{6.86 \times 10^{-4}}$
			27	**264.5**	$\mathbf{-1.3 \times 10^{5}}$	$\mathbf{1.71 \times 10^{-2}}$
P11047	**Laminin subunit gamma-1**		**4**	**248.2**	$\mathbf{-1.8 \times 10^{1}}$	$\mathbf{4.78 \times 10^{-2}}$
			4	**250.0**	$\mathbf{-1.4 \times 10^{5}}$	$\mathbf{1.54 \times 10^{-2}}$
Q14112	Nidogen-2		3	128.8	-7.8×10^{0}	9.04×10^{-2}
		Processing				
P08253	**72 kDa type IV collagenase**		**13**	**100.0**	**-1.4E+00**	$\mathbf{3.45 \times 10^{-2}}$
P07711	**Cathepsin L1**		**53**	**38.9**	$\mathbf{6.8 \times 10^{0}}$	$\mathbf{2.49 \times 10^{-2}}$
A6XNE2	Complement factor D preproprotein		45	27.6	3.6×10^{0}	7.86×10^{-2}
P01034	**Cystatin-C**		**50**	**13.7**	$\mathbf{5.1 \times 10^{0}}$	$\mathbf{7.16 \times 10^{-3}}$
P01033	**Metalloproteinase inhibitor 1**		**52**	**30.6**	$\mathbf{-3.6 \times 10^{4}}$	$\mathbf{2.72 \times 10^{-2}}$
Q15113	**Procollagen C-endopeptidase enhancer 1**		**48**	**47.1**	**2.3E+00**	$\mathbf{4.65 \times 10^{-2}}$
		Regulation/Signaling				
P11021	**78 kDa glucose-regulated protein, HSPA5 protein**		**15**	**105.5**	$\mathbf{-1.1 \times 10^{5}}$	$\mathbf{1.15 \times 10^{-2}}$
			16	104.3	2.4×10^{0}	6.44×10^{-2}
Q15848	**Adiponectin**		**9**	**33.4**	$\mathbf{2.3 \times 10^{0}}$	$\mathbf{3.09 \times 10^{-2}}$
			10	33.9	-1.4×10^{0}	8.52×10^{-2}
P02649	**Apolipoprotein E**		**8**	**38.2**	$\mathbf{2.8 \times 10^{0}}$	$\mathbf{6.77 \times 10^{-2}}$
			8	**17.6**	$\mathbf{9.3 \times 10^{0}}$	$\mathbf{1.50 \times 10^{-2}}$
			8	**37.8**	$\mathbf{-9.7 \times 10^{4}}$	$\mathbf{4.81 \times 10^{-4}}$
			8	**39.3**	$\mathbf{1.8 \times 10^{0}}$	$\mathbf{6.60 \times 10^{-3}}$
			23	**91.1**	$\mathbf{-1.6 \times 10^{4}}$	$\mathbf{7.28 \times 10^{-3}}$
P09382	Galectin-1		5	12.7	2.3×10^{0}	6.51×10^{-2}
P00738	**Haptoglobin**		**30**	**19.3**	$\mathbf{7.3 \times 10^{0}}$	$\mathbf{4.54 \times 10^{-2}}$
Q02818	**Nucleobindin-1**		**14**	**74.4**	$\mathbf{-4.4 \times 10^{0}}$	$\mathbf{3.31 \times 10^{-3}}$
P36955	Pigment epithelium-derived factor		20	51.4	-6.0×10^{0}	6.02×10^{-2}
			33	19.1	-1.6×10^{4}	5.89×10^{-2}
P05121	**Plasminogen activator inhibitor 1**		**38**	**49.8**	$\mathbf{-2.9 \times 10^{0}}$	$\mathbf{1.42 \times 10^{-3}}$
P30101	Protein disulfide-isomerase A3		25	66.9	-6.6×10^{0}	7.80×10^{-2}
P02787	**Serotransferrin**		**41**	**116.6**	$\mathbf{-1.9 \times 10^{1}}$	$\mathbf{3.84 \times 10^{-5}}$
			41	116.4	-2.9×10^{0}	8.53×10^{-2}
		Nonclassical Secreted				
P06733	**Alpha-enolase (Isoform alpha-enolase)**		**48**	**47.1**	$\mathbf{2.3 \times 10^{0}}$	$\mathbf{4.65 \times 10^{-2}}$
P09496	Clathrin light chain A *		1	32.9	4.3×10^{0}	7.93×10^{-2}

dx.doi.org/10.1021/pr300539b | J. Proteome Res. 2012, 11, 4733−4743

Table 1. continued

accession number	protein name	ID	MW [kDa]	fold change	treatment *p*-value
		Nonclassical Secreted			
Q13011	**Delta(3,5)-Delta(2,4)-dienoyl-CoA isomerase**	**46**	**33.6**	**4.1× 10^0**	**9.36 × 10^{-3}**
P09622	Dihydrolipoyl dehydrogenase	49	72.6	2.5× 10^0	9.41 × 10^{-2}
P15090	**Fatty acid-binding protein, adipocyte**	**32**	**12.9**	**1.4 × 10^2**	**3.58 × 10^{-2}**
		32	**12.9**	**8.8 × 10^1**	**3.36 × 10^{-2}**
		32	**13.0**	**3.4× 10^0**	**4.54 × 10^{-2}**
		35	**27.2**	**5.0× 10^0**	**3.03 × 10^{-2}**
P00338	**L-lactate dehydrogenase A chain**	**53**	**38.9**	**6.8× 10^0**	**2.49 × 10^{-2}**
P07195	L-lactate dehydrogenase B chain	37	49.7	−1.4× 10^0	6.62 × 10^{-2}
Q06830	Peroxiredoxin-1	51	23.6	2.6× 10^0	8.94 × 10^{-2}
P32119	**Peroxiredoxin-2**	**19**	**21.5**	**4.1E+00**	**1.83 × 10^{-2}**
P30086	**Phosphatidylethanolamine-binding protein 1**	**43**	**21.5**	**5.4E+00**	**9.55 × 10^{-3}**
P48741	Putative heat shock 70 kDa protein 7 *	16	104.3	2.4× 10^0	6.44 × 10^{-2}
P50454	**Serpin H1**	**56**	**50.0**	**−1.1 × 10^2**	**4.55 × 10^{-5}**
P00441	Superoxide dismutase [Cu−Zn]	28	18.9	3.3× 10^0	7.88 × 10^{-2}
P08670	**Vimentin**	11	49.4	−3.4× 10^0	7.78 × 10^{-2}
		11	**66.5**	**−1.4 × 10^1**	**5.78 × 10^{-3}**
		11	**61.2**	**−1.2 × 10^4**	**3.66 × 10^{-8}**
		Intracellular			
P10809	**60 kDa heat shock protein**	**22**	**74.5**	**−2.7× 10^0**	**4.98 × 10^{-2}**
Q03154	Aminoacylase-1	36	47.9	2.7× 10^0	9.53 × 10^{-2}
P60709	**Actin**	21	48.1	−2.5× 10^0	7.36 × 10^{-2}
		39	**48.7**	**−7.6× 10^0**	**3.19 × 10^{-5}**
Q9UKK9	ADP-sugar pyrophosphatase	10	33.9	−1.4× 10^0	8.52 × 10^{-2}
P00325	**Alcohol dehydrogenase 1B**	**55**	**46.8**	**4.1× 10^0**	**4.57 × 10^{-2}**
P12277	Creatine kinase B-type	21	48.1	−2.5× 10^0	7.36 × 10^{-2}
Q16555	**Dihydropyrimidinase-related protein 2**	**40**	**85.7**	**−2.7× 10^0**	**4.60 × 10^{-2}**
Q13561	Dynactin subunit 2	20	51.4	−6.0× 10^0	6.02 × 10^{-2}
P04075	**Fructose-bisphosphate aldolase A**	47	53.3	3.4× 10^0	9.96 × 10^{-2}
		47	47.2	4.9× 10^0	7.99 × 10^{-2}
		47	240.0	−2.1× 10^0	7.09 × 10^{-2}
		55	**46.8**	**4.1× 10^0**	**4.57 × 10^{-2}**
P04406	Glyceraldehyde-3-phosphate dehydrogenase	54	41.3	7.9E+00	5.79 × 10^{-2}
P08107	**Heat shock 70 kDa protein 1A/1B**	**23**	**91.1**	**-1.6 × 10^4**	**7.28 × 10^{-3}**
		24	**91.4**	**−1.9 × 10^4**	**1.72 × 10^{-3}**
P22626	**Heterogeneous nuclear ribonucleoproteins A2/B1(Isoform B1)**	**42**	**25.8**	**3.6× 10^0**	**2.85 × 10^{-2}**
P40925	Malate dehydrogenase	44	38.8	3.1× 10^0	9.36 × 10^{-2}
P15531	Nucleoside diphosphate kinase A	29	19.6	2.0× 10^0	9.42 × 10^{-2}
P30041	**Peroxiredoxin-6**	**35**	**27.2**	**5.0× 10^0**	**3.03 × 10^{-2}**
P07737	**Profilin-1**	**50**	**13.7**	**5.1× 10^0**	**7.16 × 10^{-3}**
P60174	**Triosephosphate isomerase**	**34**	**26.7**	**−6.5× 10^0**	**4.84 × 10^{-3}**
		34	**27.2**	**9.5× 10^0**	**3.13 × 10^{-2}**
O75347	Tubulin-specific chaperone A	18	9.8	3.5× 10^0	5.14 × 10^{-2}

[a]Proteins with the identical ID number were identified in the same spot and proteins marked with asterisk (*) were identified as novel adipocyte secreted proteins. Bold font lines mark proteins/protein isoforms which are significantly differentially expressed ($P < 0.05$). Regular font lines relate to a trend for change ($0.05 < P < 0.10$).

7) and proteins involved in the regulation of apoptosis (galectin-1 and haptoglobin). Both stress- and apoptosis-related proteins were significantly as well as by trend induced by RSV (Table1). In addition, peroxiredoxin 1 (by trend), peroxiredoxin 2 (significant) and superoxide dismutase (by trend), which are proteins that protect cells from radicals, peroxides and oxidative damage, were also induced by RSV. Apolipoprotein E (ApoE) and fatty acid binding protein (FABP), which are involved in TG regulation, were also significant RSV-induced. In addition, RSV mediated a down-regulation of plasminogen activator inhibitor 1 (PAI-1) (significant) and pigment epithelium-derived factor (PEDF) (by trend) and a significant up-regulation of adiponectin.

Validation of the Identified Proteins

Comparison of the RSV data set with recent human and rodent adipokine proteomics studies[14,21−30] identified clathrin light chain A and putative heat shock 70 kDa protein 7 as novel adipocyte secreted proteins. Most of the identified differentially expressed proteins are annotated as classical adipocyte secreted proteins. Since other proteomics studies on RSV-induced secretome changes are lacking we compared our data with currently existing gene and protein expression data with respect to RSV-specific effects on mouse 3T3-L1 adipocytes,[31−34] visceral adipose tissue from Zucker rats,[35] human SGBS adipocytes,[36,37] human adipose tissue explants[6] and human visceral adipocytes.[38] Within these data sets, interleukin (IL)

dx.doi.org/10.1021/pr300539b | J. Proteome Res. 2012, 11, 4733−4743

1β, 6, 8, monocyte chemotactic protein (MCP)-1, tumor necrosis factor (TNF)-α, PAI-1, peroxisome proliferator-activated receptor (PPAR)-γ, resistin, Sirt1 and visfatin were found down-regulated by RSV. Only adiponectin and once PPARγ were found to be RSV-induced.[6,31−33,35−39] Comparison with our data confirmed only adiponectin and PAI-1 expression and regulation.[6,31,33,35,38]

DISCUSSION

Obesity is associated with the development of metabolic diseases and increased mortality. Consequently, obesity has a considerable impact on personal life quality.[13,40] RSV is known to mimic beneficial effects of calorie restriction and may positively affect obesity-associated diseases.[1,3,5] Our study is the first using a proteomic approach to study the effect of RSV on the secretome of human adipocytes. The use of human SGBS adipocytes was based on the fact that human fat biopsies are limited with respect to the amount of preadipocytes and their differentiation capacity. In contrast, human preadipocytes from subcutaneous adipose tissue of an infant with Simson-Golabi-Behmel syndrome (SGBS) can display a differentiation capacity of up to 90% and retain this capacity over at least 30 generations while being morphologically, biochemically and functionally similar to primary preadipocytes.[15] In addition, Fischer-Posovszky et al.,[41] our group[14] and Luo et al.[42] showed that SGBS cell are an ideal cell model to study adipocyte biology and its secretion behavior. As such, SGBS (pre)-adipocytes are a good choice to investigate the adipocyte differentiation, manipulation and secretome. Our results show that RSV, concomitantly with reduced intracellular TG levels, positively affected the SGBS adipocyte secretion profile with respect to the obesity-associated metabolic pattern. Furthermore, two novel adipocyte-secreted proteins were discovered from which the expression was regulated by RSV.

RSV-treated adipocytes showed a significant decrease in intracellular lipid (TG) content which might be the result of increased intracellular lipolysis, as supported by an increased basal glycerol release. The intracellular lipolysis is mediated by lipase activity. As such, HSL and ATGL lipases are responsible for more than 95% of the lipase activity in human adipocytes.[43] Rayalam et al.[32] showed in 3T3-L1 adipocytes a RSV-induced SIRT1 repression of peroxisome proliferator-activated receptor gamma (PPARγ), CCAAT/enhancer binding protein α (C/EBPα), FAS and lipoprotein lipase (LPL), which is in line with inhibition of lipid accumulation in adipocytes. In addition, Lasa et al.[44] demonstrated clearly a RSV-induced lipolysis by ATGL activity in SGBS and 3T3-L1. Rayalam et al.[32] further showed a RSV-induced reduction of the HSL expression, which we also observed in the SGBS cells (Supporting Information File 2).

The use of RSV concentration of 75 μM is high compared to physiological RSV concentrations. Such high concentrations are not achieved by normal diets and also not measured in the blood plasma.[1,5,45] In addition, the bioavailability of RSV in in vivo studies is dramatically reduced due to a rapid and extensive conversion to resveratrol glucuronides and resveratrol sulfates.[46] Therefore, pharmacological intervention with high RSV concentrations might be needed to bring about the RSV-induced beneficial effects. However, Timmers et al. demonstrated at physiological RSV concentration beneficial effects on insulin sensitivity and improved blood glucose, triglycerides and cytokines levels.[5] Such in vivo studies are based on longer intervention periods.[5] In contrast, in vitro studies which mostly use cell models, have to achieve the same effects in a shorter intervention period until 96 h. This limitation requires an increased RSV concentration which was used here over a period of 48 h.

RSV of in vitro experiments was demonstrated to be oxidized after 24 h which decreases its activity and generates oxidative stress by producing H_2O_2.[47] Increased H_2O_2 levels were shown to decrease SIRT1 expression which might negatively effects the SIRT1-induced lipolysis and inhibition of lipid accumulation in adipocytes.[32] Oxidized RSV could also be the explanation of the significant decrease of the glycerol release of 5 μM RSV treated adipocytes in our study. To avoid the oxidation of RSV and in turn increased levels of oxidative stress, RSV might be protected by adding vitamin C or superoxide dismutase (SOD) to the culture medium. On the other hand, additional substances might lead to cross-reaction and a differentially expressed secretome profile. In addition, vitamin C and SOD are shown to even enhance the H_2O_2 production[48] or produce inconsistent results.[49] Therefore, no extra measures were taken to protect the RSV in the medium. To investigate the presence of functional RSV, we performed SIRT1 Western blotting of 48 h 75 μM RSV-treated or nontreated SGBS adipocytes which revealed a RSV-induced significant increase of SIRT1 expression (Supporting Information File 2). SIRT1 is thought to be indirectly activated by RSV via Epac1 and AMPK signaling pathway[10] and is down-regulated by H_2O_2 production.[50−52] Apparently, functional RSV was present to explain the measured effects including increased lipolysis and decreased TG content and secretome changes, although we cannot totally exclude H_2O_2-induced secretome affections due to oxidized RSV.

The observed RSV-induced reduction in intracellular TG content might result in a decreased adipocyte cell size and induces structural remodelling.[53,54] In line, we observed that most of structural proteins including ECM components, serpin H1 as a collagen binding protein and filament-related proteins (vimentin) are significantly down-regulated while processing proteins including cathepsin L1, cystatin-C and procollagen C-endopeptidase enhancer 1 are significantly up-regulated after RSV treatment. It has been shown that reduced expression levels of vimentin result in a decreased lipid droplet formation.[55] As such, this may explain the RSV-mediated reduction in vimentin secretion which is accompanied by decreased lipid content. Reduced cell size urges a decreased expression of cell structure proteins and complies with the lower relative abundance of ECM proteins and the up-regulation of the processing proteins allowing the remodelling of the ECM. Cell shrinking may lead to cellular stress and may eventually induce apoptosis.[53,54] Indeed, Rayalam et al.[32] reported increased apoptosis in RSV-treated 3T3-L1 adipocytes. In addition, Mader et al.[51] investigated a SIRT1-independent way of RSV-induced apoptosis in SGBS adipocytes. It was shown that RSV inhibited phosphoinositide 3 kinase-driven phosphorylation of Akt that in turn induces Bax activation. This resulted in caspase-dependent apoptosis. The present study identified apoptosis and stress-related proteins including heat shock proteins and galectin-1,[56] which were up-regulated by RSV. It confirms the occurrence of cellular stress and increases the liability toward apoptosis, mimicking the effect of calorie restriction on adipocytes.[51] Although we cannot conclude whether RSV mediates apoptosis in fat cells via cell shrinking or via a caspase-dependent pathway, our findings support the theory of RSV-induced adipocyte apoptosis. This may have implications for a potential application of RSV to

reduce fat content in obese subjects by mimicking calorie restriction and adipocyte apoptosis.

Beside the induction of stress- and apoptosis-related proteins, we observed that RSV also induced proteins that protect cells from oxidative damage like peroxiredoxin 1, 2 and superoxide dismutase. It has been shown previously that RSV treatment activates antioxidants and in turn reduces mitochondrial reactive oxygen species in human endothelial cells.[57] Peroxiredoxin (Prx) proteins are generally known to protect against oxidative stress. Prx-2 reduces generated hydrogen peroxide noncatalytically[58] while the redox function of Prx-1 is still under discussion. Kim et al.[59] demonstrated that Prx-1 is negatively correlated with the apoptosis signaling-regulating kinase 1 (ASK1) that stimulates apoptosis. On the other hand, Morinaka et al.[60] showed that high levels of oxidative stress induced the formation of oligomeric Prx-1 which leads to p53-induced cell apoptosis. Up-regulation of Prx-proteins suggests higher levels of oxidative stress which may be induced by apoptosis or increased lipolysis and up-regulated metabolic enzymes.[61] It shows that RSV-treated adipocytes react in a cell survival manner to deal with increased cellular stress.

Next to the apoptosis regulation and the antioxidative capacity of RSV on adipocytes, we identified in this study two novel adipocyte-secreted proteins. They were classified as nonclassical secreted proteins. First, clathrin light chain A is a protein of the coated pits and vesicles. As such, it is involved in accumulation of proteins on the plasma membrane like glucose transporter (GLUT) 4 in adipocytes.[62] Translocation of GLUT 4 proteins is an important regulatory mechanism of the glucose transport into the cells (adipocytes) and may play an important role in the regulation of blood circulating glucose levels. Second, the putative heat shock 70 kDa protein 7 belongs to the heat shock protein (HSP) 70 family and as such mostly associated with the stress response. Not much is known about the putative heat shock 70 kDa protein 7. However, HSP70 chaperons are ubiquitous proteins and mostly associated with adenosine triphosphate-dependent biological processes including protein folding, degradation and translocation.[63]

RSV mimics the effect of calorie restriction, which includes a less inflammatory phenotype as well as an improvement of metabolic complications.[5,64] The observed regulation patterns of adiponectin, ApoE, PAI-1 and PEDF indicate that RSV reverses the human adipocyte secretion profile toward a less inflammatory phenotype and a more insulin-sensitizing pattern. Adiponectin, ApoE, PAI-1 and PEDF are known to be involved in inflammatory processes.[65−70] Therefore, a reduced secretion of PAI-1 and PEDF and elevated secretion of the anti-inflammatory factors adiponectin and ApoE by RSV might indicate a potential anti-inflammatory effect of RSV. ApoE, which is known to regulate TG turnover as well as expression of genes which are involved in lipid synthesis to fulfill the energy and lipid homeostasis of cells, induces a conversion of pro-inflammatory M1 macrophages toward M2 macrophages with anti-inflammatory phenotypes.[67] This indicates that RSV-induced ApoE secretion might be involved in the switch between macrophage phenotypes, contributing to its anti-inflammatory effect. To the best of our knowledge, this is the first report that shows a RSV-mediated induction of ApoE secretion from human adipocytes. However, increase of ApoE secretion might also be a protection mechanism against oxidative stress which is shown by Tarnus et al.[71] Beside a possible H_2O_2 environment due to oxidized RSV, a RSV- and as such a SIRT1-induced lipolysis and in turn cell shrinking processes also cause oxidative stress.[32,51,53,54] In contrast to the finding of Tarnus et al.,[71] Esperitu et al.[72] clearly demonstrated in a H_2O_2 environment an oxidative stress-stimulated Apo-E suppression in mice adipocytes. In addition, the here observed regulation pattern of adiponectin and PAI-1 is contrary to the protein regulation pattern under H_2O_2-induced oxidative stress.[73,74] Therefore, we conclude that the Apo-E up-regulation and its anti-inflammatory actions are the result of functional RSV and its downstream signaling.

Together with the increased ApoE secretion, the RSV-induced up-regulation of adiponectin and down-regulation of PEDF (by trend) and PAI-1 indicate an adipocyte secretome profile toward a more insulin-sensitizing pattern. Adiponectin is involved in glucose regulation, fatty acid catabolism and increased insulin sensitivity. The levels of circulating adiponectin are reduced during the development of obesity, which negatively influences insulin sensitivity and in turn may lead to metabolic syndrome complications.[75] The observed up-regulation of adiponectin secretion might be a beneficial effect with respect to increased glucose uptake in muscles, insulin sensitivity and suppressed gluconeogenesis in the hepatocytes.[76] In addition, adiponectin is an anti-inflammatory factor that inhibits pro-inflammatory factors including TNF-α and reactive oxygen species.[66] The observed RSV-induced adiponectin levels are in line with recent literature,[6,31,33−35,38] although Derdemezis et al.[36] showed no RSV-stimulated adiponectin expression in SGBS adipocytes. This result was explained by the lower inflammatory characteristics of SGBS adipocyte type compared to visceral adipocytes.[36] However, the use of only 10 μM or 25 μM RSV concentration over a period of 24 and 48 h[36] might be the more reasonable explanation for the absence of RSV-stimulated effects which is also shown in our RSV concentration course study.

PEDF is associated with enlarged adipose tissue mass and insulin resistance.[77,78] Down-regulation of PEDF may be beneficial for insulin sensitivity and decreases the inflammatory phenotype within obese subjects.[65] Here all identified PEDF spots were down-regulated by trend which shows a potential regulation mechanism of PEDF during RSV treatment. As such, it is, to the best of our knowledge, the first report that shows a RSV-mediated down-regulation of PEDF secretion from human adipocytes.

PAI-1 stimulates the fibrinogen formation by inhibiting matrix metalloproteinases and fibrinolysis. Such increased fibrinogen expression is also related to low-grade inflammation.[70] As such, a down-regulation of PAI-1 may decrease the chance of development of obesity-induced thrombosis and cardiovascular diseases.[70,79] The RSV-mediated down-regulation of PAI-1 found in the present study is in-line with literature and might contribute to the potential anti-inflammatory action of RSV.[6,31,34]

■ CONCLUSION

We showed caloric-restrictive effects of RSV in human adipocytes and in turn a changed adipocyte secretion profile that indicates ECM remodelling, reduced cellular stress and modification of apoptosis sensitivity. In addition, a RSV-induced up-regulation of ApoE and adiponectin together with a down-regulation of PAI-1 and PEDF may change the adipocyte secretion profile toward a more beneficial pattern that may improve the obesity-associated pro-inflammatory state, insulin sensitivity and thrombotic phenotype.

■ ASSOCIATED CONTENT

Supporting Information

Additional material as noted in text. This material is available free of charge via the Internet at http://pubs.acs.org.

■ AUTHOR INFORMATION

Corresponding Author

*Department of Human Biology, Maastricht University, P.O. Box 616, 6200 MD Maastricht, The Netherlands. Phone: 0031 43 38 81509. Fax: 0031 43 36 70976. E-mail: a.rosenow@maastrichtuniversity.nl.

Notes

The authors declare no competing financial interest.

■ ACKNOWLEDGMENTS

We thank Freek Bouwman of the Department Human Biology, University Maastricht, The Netherlands, Eric Royackers of the Biomedical Research Institute, University Hasselt, Belgium for their practical support and Prof. Dr. Martin Wabitsch of the Endocrine Research Laboratory, Division of Pediatric Endocrinology and Diabetes, Ulm University Medical Center, Germany for the kind gift of SGBS cells.

■ REFERENCES

(1) Baur, J. A.; Pearson, K. J.; Price, N. L.; Jamieson, H. A.; Lerin, C.; Kalra, A.; Prabhu, V. V.; Allard, J. S.; Lopez-Lluch, G.; Lewis, K.; Pistell, P. J.; Poosala, S.; Becker, K. G.; Boss, O.; Gwinn, D.; Wang, M.; Ramaswamy, S.; Fishbein, K. W.; Spencer, R. G.; Lakatta, E. G.; Le Couteur, D.; Shaw, R. J.; Navas, P.; Puigserver, P.; Ingram, D. K.; de Cabo, R.; Sinclair, D. A. Resveratrol improves health and survival of mice on a high-calorie diet. *Nature* **2006**, *444* (7117), 337−42.

(2) Roemer, K.; Mahyar-Roemer, M. The basis for the chemopreventive action of resveratrol. *Drugs Today* **2002**, *38* (8), 571−80.

(3) Baur, J. A. Resveratrol, sirtuins, and the promise of a DR mimetic. *Mech. Ageing Dev.* **2010**, *131*, 261−9.

(4) Pearson, K. J.; Baur, J. A.; Lewis, K. N.; Peshkin, L.; Price, N. L.; Labinskyy, N.; Swindell, W. R.; Kamara, D.; Minor, R. K.; Perez, E.; Jamieson, H. A.; Zhang, Y.; Dunn, S. R.; Sharma, K.; Pleshko, N.; Woollett, L. A.; Csiszar, A.; Ikeno, Y.; Le Couteur, D.; Elliott, P. J.; Becker, K. G.; Navas, P.; Ingram, D. K.; Wolf, N. S.; Ungvari, Z.; Sinclair, D. A.; de Cabo, R. Resveratrol delays age-related deterioration and mimics transcriptional aspects of dietary restriction without extending life span. *Cell Metab.* **2008**, *8* (2), 157−68.

(5) Timmers, S.; Konings, E.; Bilet, L.; Houtkooper, R. H.; van de Weijer, T.; Goossens, G. H.; Hoeks, J.; van der Krieken, S.; Ryu, D.; Kersten, S.; Moonen-Kornips, E.; Hesselink, M. K.; Kunz, I.; Schrauwen-Hinderling, V. B.; Blaak, E. E.; Auwerx, J.; Schrauwen, P. Calorie restriction-like effects of 30 days of resveratrol supplementation on energy metabolism and metabolic profile in obese humans. *Cell Metab.* **2011**, *14* (5), 612−22.

(6) Olholm, J.; Paulsen, S. K.; Cullberg, K. B.; Richelsen, B.; Pedersen, S. B. Anti-inflammatory effect of resveratrol on adipokine expression and secretion in human adipose tissue explants. *Int. J. Obes.* **2010**, *34* (10), 1546−53.

(7) Howitz, K. T.; Bitterman, K. J.; Cohen, H. Y.; Lamming, D. W.; Lavu, S.; Wood, J. G.; Zipkin, R. E.; Chung, P.; Kisielewski, A.; Zhang, L. L.; Scherer, B.; Sinclair, D. A. Small molecule activators of sirtuins extend Saccharomyces cerevisiae lifespan. *Nature* **2003**, *425* (6954), 191−6.

(8) Lin, S. J.; Defossez, P. A.; Guarente, L. Requirement of NAD and SIR2 for life-span extension by calorie restriction in Saccharomyces cerevisiae. *Science* **2000**, *289* (5487), 2126−8.

(9) Park, C. E.; Kim, M. J.; Lee, J. H.; Min, B. I.; Bae, H.; Choe, W.; Kim, S. S.; Ha, J. Resveratrol stimulates glucose transport in C2C12 myotubes by activating AMP-activated protein kinase. *Exp. Mol. Med.* **2007**, *39* (2), 222−9.

(10) Park, S. J.; Ahmad, F.; Philp, A.; Baar, K.; Williams, T.; Luo, H.; Ke, H.; Rehmann, H.; Taussig, R.; Brown, A. L.; Kim, M. K.; Beaven, M. A.; Burgin, A. B.; Manganiello, V.; Chung, J. H. Resveratrol ameliorates aging-related metabolic phenotypes by inhibiting cAMP phosphodiesterases. *Cell* **2012**, *148* (3), 421−33.

(11) Gregoire, F. M. Adipocyte differentiation: from fibroblast to endocrine cell. *Exp. Biol. Med.* **2001**, *226* (11), 997−1002.

(12) Lehr, S.; Hartwig, S.; Sell, H. Adipokines: A treasure trove for the discovery of biomarkers for metabolic disorders. *Proteomics: Clin. Appl.* **2012**, *6* (1−2), 91−101.

(13) Diamanti-Kandarakis, E.; Palioura, E.; Kandarakis, S. A.; Koutsilieris, M. The Impact of Endocrine Disruptors on Endocrine Targets. *Horm. Metab. Res.* **2010**, *42* (8), 543−52.

(14) Rosenow, A.; Arrey, T. N.; Bouwman, F. G.; Noben, J. P.; Wabitsch, M.; Mariman, E. C.; Karas, M.; Renes, J. Identification of novel human adipocyte secreted proteins by using SGBS cells. *J. Proteome Res.* **2010**, *9*, 5389−401.

(15) Wabitsch, M.; Brenner, R. E.; Melzner, I.; Braun, M.; Moller, P.; Heinze, E.; Debatin, K. M.; Hauner, H. Characterization of a human preadipocyte cell strain with high capacity for adipose differentiation. *Int. J. Obes. Relat. Metab. Disord.* **2001**, *25* (1), 8−15.

(16) Bouwman, F.; Renes, J.; Mariman, E. A combination of protein profiling and isotopomer analysis using matrix-assisted laser desorption/ionization-time of flight mass spectrometry reveals an active metabolism of the extracellular matrix of 3T3-L1 adipocytes. *Proteomics* **2004**, *4* (12), 3855−63.

(17) Dumont, D.; Noben, J. P.; Moreels, M.; Vanderlocht, J.; Hellings, N.; Vandenabeele, F.; Lambrichts, I.; Stinissen, P.; Robben, J. Characterization of mature rat oligodendrocytes: a proteomic approach. *J. Neurochem.* **2007**, *102* (2), 562−76.

(18) Barsnes, H.; Vizcaino, J. A.; Eidhammer, I.; Martens, L. PRIDE Converter: making proteomics data-sharing easy. *Nat. Biotechnol.* **2009**, *27* (7), 598−9.

(19) Vizcaino, J. A.; Cote, R.; Reisinger, F.; Barsnes, H.; Foster, J. M.; Rameseder, J.; Hermjakob, H.; Martens, L. The Proteomics Identifications database: 2010 update. *Nucleic Acids Res.* **2010**, *38* (Database issue), D736−42.

(20) Wang, R.; Fabregat, A.; Rios, D.; Ovelleiro, D.; Foster, J. M.; Cote, R. G.; Griss, J.; Csordas, A.; Perez-Riverol, Y.; Reisinger, F.; Hermjakob, H.; Martens, L.; Vizcaino, J. A. PRIDE Inspector: a tool to visualize and validate MS proteomics data. *Nat. Biotechnol.* **2012**, *30* (2), 135−7.

(21) Lehr, S.; Hartwig, S.; Lamers, D.; Famulla, S.; Muller, S.; Hanisch, F. G.; Cuvelier, C.; Ruige, J.; Eckardt, K.; Ouwens, D. M.; Sell, H.; Eckel, J. Identification and validation of novel adipokines released from primary human adipocytes. *Mol. Cell. Proteomics* **2012**, *11* (1), M111 010504.

(22) Alvarez-Llamas, G.; Szalowska, E.; de Vries, M. P.; Weening, D.; Landman, K.; Hoek, A.; Wolffenbuttel, B. H.; Roelofsen, H.; Vonk, R. J. Characterization of the human visceral adipose tissue secretome. *Mol. Cell. Proteomics* **2007**, *6* (4), 589−600.

(23) Chen, X.; Cushman, S. W.; Pannell, L. K.; Hess, S. Quantitative proteomic analysis of the secretory proteins from rat adipose cells using a 2D liquid chromatography-MS/MS approach. *J. Proteome Res.* **2005**, *4* (2), 570−7.

(24) Kim, J.; Choi, Y. S.; Lim, S.; Yea, K.; Yoon, J. H.; Jun, D. J.; Ha, S. H.; Kim, J. W.; Kim, J. H.; Suh, P. G.; Ryu, S. H.; Lee, T. G. Comparative analysis of the secretory proteome of human adipose stromal vascular fraction cells during adipogenesis. *Proteomics* **2010**, *10* (3), 394−405.

(25) Molina, H.; Yang, Y.; Ruch, T.; Kim, J. W.; Mortensen, P.; Otto, T.; Nalli, A.; Tang, Q. Q.; Lane, M. D.; Chaerkady, R.; Pandey, A. Temporal profiling of the adipocyte proteome during differentiation using a five-plex SILAC based strategy. *J. Proteome Res.* **2009**, *8* (1), 48−58.

(26) Zhong, J.; Krawczyk, S. A.; Chaerkady, R.; Huang, H.; Goel, R.; Bader, J. S.; Wong, G. W.; Corkey, B. E.; Pandey, A. Temporal

profiling of the secretome during adipogenesis in humans. *J. Proteome Res.* **2010**, *9* (10), 5228−38.
(27) Zvonic, S.; Lefevre, M.; Kilroy, G.; Floyd, Z. E.; DeLany, J. P.; Kheterpal, I.; Gravois, A.; Dow, R.; White, A.; Wu, X.; Gimble, J. M. Secretome of primary cultures of human adipose-derived stem cells: modulation of serpins by adipogenesis. *Mol. Cell. Proteomics* **2007**, *6* (1), 18−28.
(28) Chiellini, C.; Cochet, O.; Negroni, L.; Samson, M.; Poggi, M.; Ailhaud, G.; Alessi, M. C.; Dani, C.; Amri, E. Z. Characterization of human mesenchymal stem cell secretome at early steps of adipocyte and osteoblast differentiation. *BMC Mol. Biol.* **2008**, *9*, 26.
(29) Lim, J. M.; Sherling, D.; Teo, C. F.; Hausman, D. B.; Lin, D.; Wells, L. Defining the regulated secreted proteome of rodent adipocytes upon the induction of insulin resistance. *J. Proteome Res.* **2008**, *7* (3), 1251−63.
(30) Roelofsen, H.; Dijkstra, M.; Weening, D.; de Vries, M. P.; Hoek, A.; Vonk, R. J. Comparison of isotope-labeled amino acid incorporation rates (CILAIR) provides a quantitative method to study tissue secretomes. *Mol. Cell. Proteomics* **2009**, *8* (2), 316−24.
(31) Ahn, J.; Lee, H.; Kim, S.; Ha, T. Resveratrol inhibits TNF-alpha-induced changes of adipokines in 3T3-L1 adipocytes. *Biochem. Biophys. Res. Commun.* **2007**, *364* (4), 972−7.
(32) Rayalam, S.; Yang, J. Y.; Ambati, S.; Della-Fera, M. A.; Baile, C. A. Resveratrol induces apoptosis and inhibits adipogenesis in 3T3-L1 adipocytes. *Phytother. Res* **2008**, *22* (10), 1367−71.
(33) Kang, L.; Heng, W.; Yuan, A.; Baolin, L.; Fang, H. Resveratrol modulates adipokine expression and improves insulin sensitivity in adipocytes: relative to inhibition of inflammatory responses. *Biochimie* **2010**, *92* (7), 786−96.
(34) Yen, G. C.; Chen, Y. C.; Chang, W. T.; Hsu, C. L. Effects of polyphenolic compounds on tumor necrosis factor-alpha (TNF-alpha)-induced changes of adipokines and oxidative stress in 3T3-L1 adipocytes. *J. Agric. Food Chem.* **2011**, *59* (2), 546−51.
(35) Rivera, L.; Moron, R.; Zarzuelo, A.; Galisteo, M. Long-term resveratrol administration reduces metabolic disturbances and lowers blood pressure in obese Zucker rats. *Biochem. Pharmacol.* **2009**, *77* (6), 1053−63.
(36) Derdemezis, C. S.; Kiortsis, D. N.; Tsimihodimos, V.; Petraki, M. P.; Vezyraki, P.; Elisaf, M. S.; Tselepis, A. D. Effect of plant polyphenols on adipokine secretion from human SGBS adipocytes. *Biochem. Res. Int.* **2011**, *2011*, 285618.
(37) Fischer-Posovszky, P.; Kukulus, V.; Tews, D.; Unterkircher, T.; Debatin, K. M.; Fulda, S.; Wabitsch, M. Resveratrol regulates human adipocyte number and function in a Sirt1-dependent manner. *Am. J. Clin. Nutr.* **2010**, *92* (1), 5−15.
(38) Costa Cdos, S.; Rohden, F.; Hammes, T. O.; Margis, R.; Bortolotto, J. W.; Padoin, A. V.; Mottin, C. C.; Guaragna, R. M. Resveratrol upregulated SIRT1, FOXO1, and adiponectin and downregulated PPARgamma1−3 mRNA expression in human visceral adipocytes. *Obes. Surg.* **2011**, *21* (3), 356−61.
(39) Ahn, J.; Cho, I.; Kim, S.; Kwon, D.; Ha, T. Dietary resveratrol alters lipid metabolism-related gene expression of mice on an atherogenic diet. *J. Hepatol.* **2008**, *49* (6), 1019−28.
(40) Dixon, J. B. The effect of obesity on health outcomes. *Mol. Cell. Endocrinol.* **2010**, *316* (2), 104−8.
(41) Fischer-Posovszky, P.; Newell, F. S.; Wabitsch, M.; Tornqvist, H. E. Human SGBS cells—a unique tool for studies of human fat cell biology. *Obes. Facts* **2008**, *1* (4), 184−9.
(42) Luo, X.; Hutley, L. J.; Webster, J. A.; Kim, Y. H.; Liu, D. F.; Newell, F. S.; Widberg, C. H.; Bachmann, A.; Turner, N.; Schmitz-Peiffer, C.; Prins, J. B.; Yang, G. S.; Whitehead, J. P. Identification of BMP and activin membrane-bound inhibitor (BAMBI) as a potent negative regulator of adipogenesis and modulator of autocrine/paracrine adipogenic factors. *Diabetes* **2012**, *61* (1), 124−36.
(43) Schweiger, M.; Schreiber, R.; Haemmerle, G.; Lass, A.; Fledelius, C.; Jacobsen, P.; Tornqvist, H.; Zechner, R.; Zimmermann, R. Adipose triglyceride lipase and hormone-sensitive lipase are the major enzymes in adipose tissue triacylglycerol catabolism. *J. Biol. Chem.* **2006**, *281* (52), 40236−41.
(44) Lasa, A.; Schweiger, M.; Kotzbeck, P.; Churruca, I.; Simon, E.; Zechner, R.; Portillo, M. D. Resveratrol regulates lipolysis via adipose triglyceride lipase. *J. Nutr. Biochem.* **2012**, *23* (4), 379−84.
(45) Lagouge, M.; Argmann, C.; Gerhart-Hines, Z.; Meziane, H.; Lerin, C.; Daussin, F.; Messadeq, N.; Milne, J.; Lambert, P.; Elliott, P.; Geny, B.; Laakso, M.; Puigserver, P.; Auwerx, J. Resveratrol improves mitochondrial function and protects against metabolic disease by activating SIRT1 and PGC-1alpha. *Cell* **2006**, *127* (6), 1109−22.
(46) Wenzel, E.; Somoza, V. Metabolism and bioavailability of trans-resveratrol. *Mol. Nutr. Food Res.* **2005**, *49* (5), 472−81.
(47) Yang, N. C.; Lee, C. H.; Song, T. Y. Evaluation of resveratrol oxidation in vitro and the crucial role of bicarbonate ions. *Biosci. Biotechnol. Biochem.* **2010**, *74* (1), 63−8.
(48) Wee, L. M.; Long, L. H.; Whiteman, M.; Halliwell, B. Factors affecting the ascorbate- and phenolic-dependent generation of hydrogen peroxide in Dulbecco's Modified Eagles Medium. *Free Radical Res.* **2003**, *37* (10), 1123−30.
(49) Hou, Z.; Sang, S.; You, H.; Lee, M. J.; Hong, J.; Chin, K. V.; Yang, C. S. Mechanism of action of (-)-epigallocatechin-3-gallate: auto-oxidation-dependent inactivation of epidermal growth factor receptor and direct effects on growth inhibition in human esophageal cancer KYSE 150 cells. *Cancer Res.* **2005**, *65* (17), 8049−56.
(50) Bai, S. W.; Herrera-Abreu, M. T.; Rohn, J. L.; Racine, V.; Tajadura, V.; Suryavanshi, N.; Bechtel, S.; Wiemann, S.; Baum, B.; Ridley, A. J. Identification and characterization of a set of conserved and new regulators of cytoskeletal organization, cell morphology and migration. *BMC Biol.* **2011**, *9*, 54.
(51) Mader, I.; Wabitsch, M.; Debatin, K. M.; Fischer-Posovszky, P.; Fulda, S. Identification of a novel proapoptotic function of resveratrol in fat cells: SIRT1-independent sensitization to TRAIL-induced apoptosis. *FASEB J.* **2010**, *24* (6), 1997−2009.
(52) Furukawa, A.; Tada-Oikawa, S.; Kawanishi, S.; Oikawa, S. H2O2 accelerates cellular senescence by accumulation of acetylated p53 via decrease in the function of SIRT1 by NAD+ depletion. *Cell. Physiol. Biochem.* **2007**, *20* (1−4), 45−54.
(53) Mariman, E. C. An adipobiological model for weight regain after weight Loss. *Adipobiology* **2011**, 3.
(54) Mariman, E. C.; Wang, P. Adipocyte extracellular matrix composition, dynamics and role in obesity. *Cell. Mol. Life Sci.* **2010**, *67* (8), 1277−92.
(55) Lieber, J. G.; Evans, R. M. Disruption of the vimentin intermediate filament system during adipose conversion of 3T3-L1 cells inhibits lipid droplet accumulation. *J. Cell Sci.* **1996**, *109* (Pt 13), 3047−58.
(56) Hsu, D. K.; Yang, R. Y.; Liu, F. T. Galectins in apoptosis. *Methods Enzymol.* **2006**, *417*, 256−73.
(57) Ungvari, Z.; Labinskyy, N.; Mukhopadhyay, P.; Pinto, J. T.; Bagi, Z.; Ballabh, P.; Zhang, C.; Pacher, P.; Csiszar, A. Resveratrol attenuates mitochondrial oxidative stress in coronary arterial endothelial cells. *Am. J. Physiol.: Heart Circ. Physiol.* **2009**, *297* (5), H1876−81.
(58) Low, F. M.; Hampton, M. B.; Peskin, A. V.; Winterbourn, C. C. Peroxiredoxin 2 functions as a noncatalytic scavenger of low-level hydrogen peroxide in the erythrocyte. *Blood* **2007**, *109* (6), 2611−7.
(59) Kim, S. Y.; Kim, T. J.; Lee, K. Y. A novel function of peroxiredoxin 1 (Prx-1) in apoptosis signal-regulating kinase 1 (ASK1)-mediated signaling pathway. *FEBS Lett.* **2008**, *582* (13), 1913−8.
(60) Morinaka, A.; Funato, Y.; Uesugi, K.; Miki, H. Oligomeric peroxiredoxin-I is an essential intermediate for p53 to activate MST1 kinase and apoptosis. *Oncogene* **2011**, *30* (40), 4208−18.
(61) Harman, D. Aging: a theory based on free radical and radiation chemistry. *J. Gerontol.* **1956**, *11* (3), 298−300.
(62) Huang, S.; Lifshitz, L. M.; Jones, C.; Bellve, K. D.; Standley, C.; Fonseca, S.; Corvera, S.; Fogarty, K. E.; Czech, M. P. Insulin stimulates membrane fusion and GLUT4 accumulation in clathrin coats on adipocyte plasma membranes. *Mol. Cell. Biol.* **2007**, *27* (9), 3456−69.

(63) Kampinga, H. H.; Craig, E. A. The HSP70 chaperone machinery: J proteins as drivers of functional specificity. *Nat. Rev. Mol. Cell Biol.* **2010**, *11* (8), 579−92.
(64) Baur, J. A.; Sinclair, D. A. Therapeutic potential of resveratrol: the in vivo evidence. *Nat. Rev. Drug Discovery* **2006**, *5* (6), 493−506.
(65) Famulla, S.; Lamers, D.; Hartwig, S.; Passlack, W.; Horrighs, A.; Cramer, A.; Lehr, S.; Sell, H.; Eckel, J. Pigment epithelium-derived factor (PEDF) is one of the most abundant proteins secreted by human adipocytes and induces insulin resistance and inflammatory signaling in muscle and fat cells. *Int. J. Obes.* **2011**, *35* (6), 762−72.
(66) Mandal, P.; Park, P. H.; McMullen, M. R.; Pratt, B. T.; Nagy, L. E. The anti-inflammatory effects of adiponectin are mediated via a heme oxygenase-1-dependent pathway in rat Kupffer cells. *Hepatology* **2010**, *51* (4), 1420−9.
(67) Baitsch, D.; Bock, H. H.; Engel, T.; Telgmann, R.; Muller-Tidow, C.; Varga, G.; Bot, M.; Herz, J.; Robenek, H.; von Eckardstein, A.; Nofer, J. R. Apolipoprotein E induces antiinflammatory phenotype in macrophages. *Arterioscler., Thromb., Vasc. Biol.* **2011**, *31* (5), 1160−8.
(68) Odrowaz-Sypniewska, G. Markers of pro-inflammatory and pro-thrombotic state in the diagnosis of metabolic syndrome. *Adv. Med. Sci.* **2007**, *52*, 246−50.
(69) Wang, J. J.; Zhang, S. X.; Mott, R.; Chen, Y.; Knapp, R. R.; Cao, W.; Ma, J. X. Anti-inflammatory effects of pigment epithelium-derived factor in diabetic nephropathy. *Am. J. Physiol.: Renal Physiol.* **2008**, *294* (5), F1166−73.
(70) Nieuwdorp, M.; Stroes, E. S.; Meijers, J. C.; Buller, H. Hypercoagulability in the metabolic syndrome. *Curr. Opin. Pharmacol.* **2005**, *5* (2), 155−9.
(71) Tarnus, E.; Wassef, H.; Carmel, J. F.; Rondeau, P.; Roche, M.; Davignon, J.; Bernier, L.; Bourdon, E. Apolipoprotein E limits oxidative stress-induced cell dysfunctions in human adipocytes. *FEBS Lett.* **2009**, *583* (12), 2042−8.
(72) Espiritu, D. J.; Mazzone, T. Oxidative stress regulates adipocyte apolipoprotein e and suppresses its expression in obesity. *Diabetes* **2008**, *57* (11), 2992−8.
(73) Chen, B.; Lam, K. S.; Wang, Y.; Wu, D.; Lam, M. C.; Shen, J.; Wong, L.; Hoo, R. L.; Zhang, J.; Xu, A. Hypoxia dysregulates the production of adiponectin and plasminogen activator inhibitor-1 independent of reactive oxygen species in adipocytes. *Biochem. Biophys. Res. Commun.* **2006**, *341* (2), 549−56.
(74) Yu, B.; Cook, C.; Santanam, N. The aporphine alkaloid boldine induces adiponectin expression and regulation in 3T3-L1 cells. *J. Med. Food* **2009**, *12* (5), 1074−83.
(75) Kadowaki, T.; Yamauchi, T.; Kubota, N.; Hara, K.; Ueki, K.; Tobe, K. Adiponectin and adiponectin receptors in insulin resistance, diabetes, and the metabolic syndrome. *J. Clin. Invest.* **2006**, *116* (7), 1784−92.
(76) Sharma, A. M.; Chetty, V. T. Obesity, hypertension and insulin resistance. *Acta Diabetol.* **2005**, *42* (Suppl 1), S3−8.
(77) Wang, P.; Smit, E.; Brouwers, M. C.; Goossens, G. H.; van der Kallen, C. J.; van Greevenbroek, M. M.; Mariman, E. C. Plasma pigment epithelium-derived factor is positively associated with obesity in Caucasian subjects, in particular with the visceral fat depot. *Eur. J. Endocrinol.* **2008**, *159* (6), 713−8.
(78) Borg, M. L.; Andrews, Z. B.; Duh, E. J.; Zechner, R.; Meikle, P. J.; Watt, M. J. Pigment epithelium-derived factor regulates lipid metabolism via adipose triglyceride lipase. *Diabetes* **2011**, *60* (5), 1458−66.
(79) Skurk, T.; Hauner, H. Obesity and impaired fibrinolysis: role of adipose production of plasminogen activator inhibitor-1. *Int. J. Obes. Relat. Metab. Disord.* **2004**, *28* (11), 1357−64.